

KFKI-1986-34/C

COMET HALLEY: NUCLEUS AND JETS
(RESULTS OF THE VEGA MISSION)

Hungarian Academy of Sciences

**CENTRAL
RESEARCH
INSTITUTE FOR
PHYSICS**

BUDAPEST

COMET HALLEY: NUCLEUS AND JETS (RESULTS OF THE VEGA MISSION)

R.Z. SAGDEEV, G.A. AVANESOV, I.V. BARINOV, A.I. DEBABOV,
V.A. KVASIKOV, V.I. MOROZ, V.A. SHAMIS, V.I. TARNAPOLSKI,
D.A. USIKOV, Ya.L. ZIMAN, B.S. ZHUKOV

Space Research Institute,
Profsoyuznaya 84/32, 117810 Moscow GSP-7, USSR

F. SZABÓ, K. SZEGŐ, B.A. SMITH*, A. KONDOR, S. LARSON*, E. MERÉNYI,
L. SZABÓ, I. TÓTH, L. VÁRHALMI

Central Research Institute for Physics
H-1525 Budapest 114, P.O.B.49, Hungary

* also Lunar and Planetary Laboratory, University of Arizona,
Tucson, Arizona, USA

P. CRUVELLIER, A. ABERGEL, J.-L. BERTAUX, J. BLAMONT
Service d'Aéronomie Spatiale CNRS, 13012 Marseille, France

M. DANZ, D. MÖHLMAN, H. STILLER, H.P. ZAPFE
Space Research Institute, Berlin, GDR

ABSTRACT

The VEGA-1 and VEGA-2 spacecraft made their closest approach to Comet Halley on 6 and 9 March, respectively. In this paper those results of the onboard imaging experiment which were obtained around closest approach are discussed. The nucleus of the comet was clearly identifiable as an irregularly shaped object, with overall dimensions of $(16 \pm 1) \times (8 \pm 1) \times (8 \pm 1)$ km. The nucleus rotates in the prograde sense about an axis nearly perpendicular to the orbital plane with a period of 53 ± 2 hours. Its albedo is only 0.04 ± 0.02 . Many of the jet features observed during the second fly-by have been mostly spatially reconstructed. These sources form a quasi-linear structure on the surface. The dust above the surface is shown to be generally optically thin with the exception of certain specific dust jets. Brightness features on the surface are clearly seen. Correlating our data with other measurements we conclude that the dirty snow-ball model will probably need to be revised.

АННОТАЦИЯ

Наибольшего сближения с кометой Галлея космические аппараты ВЕГА-1 и ВЕГА-2 достигли 6 и 9 марта соответственно. В статье приводятся результаты, полученные с помощью телевизионной системы в непосредственной близости к комете. Однозначно идентифицировано ядро кометы, имеющее неправильную форму с основными размерами $(16 \pm 1) \times (8 \pm 1) \times (8 \pm 1)$ км. Ядро совершает оборот вокруг своей оси, почти перпендикулярной плоскости траектории, за 53 ± 2 часа. Альbedo ядра составляет $0,04 \pm 0,02 - 0,01$. Удалось воспроизвести пространственную модель большинства пылевых джетов, обнаруженных во время сближения с кометой второго КА ВЕГА. Джеты на поверхности ядра образуют структуру в виде линий. Установлено, что пыль над поверхностью, за исключением окружения джетов, оптически тонкая. Четко наблюдались изменения света на поверхности. Сопоставив полученные нами результаты с другими данными, мы пришли к выводу, что в ближайшем будущем, по всей вероятности, придется ввести коррекции в модель, описывающую ядро кометы как "грязный снежный ком".

KIVONAT

A VEGA-1 és VEGA-2 űrhajó március 6-án és 9-én közelítette meg legjobban a Halley üstököst. E cikkben a fedélzeti televíziós rendszer azon eredményeit foglaljuk össze, amelyek az üstökös közvetlen közeléből származnak. Az üstökös magját világosan azonosítottuk. Ez egy szabálytalan alakú test, amelynek fő méretei $(16 \pm 1) \times (8 \pm 1) \times (8 \pm 1)$ km. A mag 53 ± 2 óra alatt fordul meg tengelye körül, amely csaknem merőleges a pályasíkra. A mag albedója $0,04 \pm 0,02 - 0,01$. A második megközelítés alkalmával készített képeken megfigyelt jet-jelenségek többségét térbelileg rekonstruáltuk. Ezek a források egy vonalszerű képződményt alkotnak a felszínen. Megmutattuk, hogy a felszín feletti por általában optikailag vékony, leszámítva a por jetek környezetét. Fényváltások világosan megfigyelhetők a felszínen. Egybevetve adatainkat más eredményekkel, arra a következtetésre jutottunk, hogy a "piszkos hógolyó"-modellt a közeljövőben valószínűleg módosítani kell.

INTRODUCTION

One of the main scientific objectives of the Vega mission was to accomplish studies of the nucleus and its immediate environment, including visual imaging of this zone and of the nucleus itself. The device dedicated to this task was the on-board television system (TVS) of the spacecraft. As the probes Vega-1 and Vega-2 were three-axis stabilized and at closest approach the relative speed of the s/c to comet was high, 79.222 km/sec and 76.785 km/sec respectively, TVS was put on a steerable pointing platform which operated under the automatic control of the TVS.

The TVS itself has two telescopes, a wide angle (focal length 150 mm) used only for navigation during the actual encounter and a narrow angle Ritchey-Chretien (focal length 1200 mm). In each telescope the light path was split into two beams before reaching the 512x512 pixel CCD detectors. The resolution was 24.8x33 and 3.4x4.1 arc sec, respectively. In front of one of the CCDs in the narrow angle camera, there was a filter magazin with 5 wide band and one narrow band filters to cover the 400-1100 Å range; the other channels had fixed filters. The description of the TVS and its various operating modes has been published earlier /1/ the more important technical characteristics are summarized in Table 1.

The power and telemetry allocated for TVS made it possible to observe the comet for two hours, from -14, -7, +7, +14 million km and for three hours around closest approach. Some of the observation windows were not used because of technical reasons. To economize the telemetry, there were several options to send back images to Earth. During the actual encounter we used almost exclusively only two: either the whole 512x512 frame or a 128x128 pixel "moving window" around the nucleus was transmitted. The center of the moving window and the exposure time was set automatically by the on-board processors, the sequence of the filters (photo-sequences) was preselected before launch and fixed in memory. There was a further option to define additional photo sequences by ground commands. We took advantage of this capability several times. Occasionally, the automatic exposure time was overridden to get better details of an overexposed center. Housekeeping data were also relayed to ground.

Before launch the system underwent appropriate ground calibration. The temperature dependence of the dark current and different transfer functions (spectral, point, line) were measured; it was established that the charge transfer efficiency is better than 0.9997/line, the pixel-to-pixel sensitivity (flat field) was recorded in different spectral bands at different exposure times; and the linearity of the detectors was evaluated as well as the angular resolution of the system, using a special grid pattern. An example of these measurements, the spectral response function is shown in Figure 1.

Provision was made for in-flight calibration as well. Until mid-February 1986, the pointing platform was in retracted position, and built-in calibration lamps were used to check the response of the system every other month. After putting the platform into the operational position, Jupiter and Saturn were observed several times before and after encounter, both to check the operation and to obtain baseline data for the photometric analysis of the comet.

In the following chapter we summarize the data-analysis accomplished since publishing the first, preliminary results /2/ and in chapter 3 we summarize the most important results relating to the nucleus of Comet Halley and conclude with a coherent description of it.

DATA ANALYSIS

1. The data we are using here were obtained by Vega-1 (2) on 6(9) March 1986 around closest approach at 7 h 20:06 UT (7 h 20:06 UT) at a minimum distance of 8889 km (8030 km). In the case of V-1, small (128x128 pixel) images were relayed to Earth approximately every 20 sec, for V-2, due to an on-board malfunction, we had to send commands to transmit full-frame (512x512 pixel) images at a rate of about one each 90 sec. The projection of the V-2 path onto a sphere centered on the nucleus is shown in Figure 2, with the recording of individual images indicated. The flight-path of V-1 was similar but about 3° further to ecliptic North. In all these images the phase angle is less than 90°; this is in contrast to Giotto's HMC /8/ where the phase angle was greater than 90°. The quality of the images is generally good, but two problems should be mentioned: a.) On V-1, as in-flight calibration data has shown, an offset of unknown cause appeared in the output signal; thus, only intensities higher than a certain threshold were digitized and transmitted.

b.) Both the V-1 and V-2 images exhibited some noise, possibly of different origin. Although this noise interferes with the data, different efforts including Fourier transformation are being tried to remove or to suppress the coherent components. Preliminary results are encouraging.

Images were taken through several spectral filters. At the present state of analysis, no significant differences have been observed in different spectral bands.

In the following discussion we call "preprocessed" images (PPI) those, which are at least partially corrected for calibration and noise.

2. The first of our goals was to deduce the size and rotation of the nucleus. To do so, several types of analyses have been applied to the preprocessed images, exhibited in Figures 3 and 4 for two different cases.

a) The maximum-gradient technique. After defining the center of the image, local gradients were attached along a number of different directions from the center to each pixel. The maximum of the local gradients along each direction was then selected. By introducing a small deviation from the maximum, a narrow contour could be obtained, within which it is believed the true limb is to be found (Figure 3a and 4a.)

b) Texture enhancement. First, a 15x15 matrix with each element set equal to 1, was passed through each image I, producing a low-pass filtered version L which is then subtracted to give $T=I-L$. By enhancing T, T_1 was obtained, and $I_1=T_1+L$ was created. (Figure 3b, 4b.). The suspected nucleus itself appears as the black region in the center of the images.

c) The above mentioned mathematical techniques should work well for the illuminated part of an unobscured celestial object. However, dust and jets distort the photometry of the nucleus, and at this stage their effect can only be corrected through the intelligence and skill of the experimenter, by iterating among different images. The unilluminated regions beyond an irregular terminator must also be taken into account to get the correct contour. This also requires iteration among images, a good understanding of the flight geometry and perhaps a certain amount of intuition. The corrected contours are shown in Figure 3c, 4c. Images on Figure 3 and 4 are not correct for aspect ratio (i.e. no correction was made for the rectangular pixels. The preprocessed but aspect corrected images are shown in Figure 5. The above considerations have led us to conclude that the overall size of the nucleus is $(16\pm 1)\times(8\pm 1)\times(8\pm 1)$ km. The comparison of the geometrical position of the nucleus during the V-1 and V-2 encounter has made it possible to decrease the uncertainties of rotation period given earlier /2/ to a present value of 53 ± 2 h. Direct rotation is assumed; retrograde rotation would give a period completely inconsistent with other estimates. We have also obtained a solution for the orientation of the rotation axis, pairing together V-1 and V-2 images, such that the nucleus is seen along both major and minor axes. It was assumed that, in each case, a plane perpendicular to the minimal inertial axis and going through the center of mass of each image should contain the rotation axis. The line defined by the intersecting planes gives its true position in space. Our present estimate is that the rotation axis is nearly perpendicular to the orbital plane, although perhaps slightly shifted in the direction of the ecliptic pole within 5° or 10°. This position is also the most likely from considerations of solar tidal perturbations.

3. To obtain better limb fits, an understanding of the 3-dimensional jet-pattern was important. A detailed analysis is reported elsewhere /3/; here the results are summarized. The analysis was done only for the V-2 encounter, because full-frame images and the absence of the intensity offset made it easier to define the jet cores and their boundaries. A typical raw image of the set used is shown in Figure 6. To get the 3-d reconstruction, we assumed that the jet sources could be approximated by either discrete points or lines, since two edges of a linear source should generally be distinguishable on several of the images. With these assumptions many (but not all) of the features were spatially reconstructed. The results are shown in Figure 1. One important discovery is that not only are many of the sources actually pointlike or linear, but that they seem to be ordered to form an even larger quasi-linear structure along the surface.

One part of this long source crosses the projection of the s/c trajectory, and V-2 should have crossed it shortly after closest approach. This is confirmed by the SP-1 dust-counter data which detected it between 7h 20:30 - 21:00 UT /4/ and partly by the general diffuse nature of dust jets seen in the image taken at 7h 21:38 UT.

4. An important question which requires a definitive answer is whether we saw the nucleus itself or just a dust cocoon surrounding it. Not only is the question of scientific importance, but there is a need to set straight the remarks of certain untrained observers (and even some experts) present in Moscow during the encounter. First we have to analyse how dust can alter surface observation.

It is known that immediately above the surface of the cometary nucleus there is some boundary layer, inside of which velocity of the dust particles is increasing with height. Near the surface the velocity of particles is almost zero and increasing at a rate proportional to the square root of the height, at height ~ 1 km it is equal to 80 or 90% of terminal value /5/. Consequently the number density of the dust particles near the surface can be large and the dust boundary layer can in principle screen the surface and even make it invisible. Three cases are possible where τ is the vertical optical thickness of the boundary layer:

- A. $\tau \leq 0.1$. Surface features can be seen.
- B. $0.1 \leq \tau \leq 1.0$. Surface features are strongly masked by dust, but some of them may be seen with difficulty
- C. $\tau \geq 1.0$. Only dust boundary layer is seen.

In modeling the photometric properties of the system consisting both of the surface and a geometrically thin and (to a first approximation) horizontally homogeneous scattering and absorbing dust layer, a comparison can be made with the observed photometric properties and thus allow discrimination among cases A, B, C.

For the surface, it is assumed that the angular dependence of the brightness factor $\rho = \pi B / E_0$, where B is the brightness and E_0 is the normal illuminance, is the same as for the Moon; the absolute values, however, will be normalized to the measured numbers.

The analysis consists of two types of photometric data: the profile of ρ for a given phase angle (Figure 7,8) and the phase curve (Figure 9). Note that this particular phase curve is not the conventional phase dependence, expressed in stellar magnitudes, of the disk-integrated brightness, but rather is the phase curve of the brightest part of the image. This is assumed to be the subsolar point of the nucleus, where incident angle $i=0$ and emission angle e is equal to the phase angle α .

For the dust, we assume a single scattering albedo, $a = 0.5$. This is the minimal possible value for large particles with $2\pi r/\lambda \gg 1$, where r is the radius of the scattering particles and λ is the wavelength. Measurements in situ on VEGA-2 /4,6/ and Giotto /7/ lead to the conclusion that such large particles dominate in the scattering and extinction of light.

From conventional radiative transfer methods, models can be generated for a variety of optical depths (Figure 8). It can be seen that the smallest optical depth (0.1) gives the best fit. However it should be noted that the shape of the profile for $\tau=2$ fits well if the intensity were decreased by a factor of two, a comparison that might be made if the absolute VEGA-2 calibration were in error by an equivalent factor. Other values for τ can be rejected because of the sharp peak near the illuminated limb, a feature not seen in the VEGA images. Finally, the case for $\tau=2$ with renormalized intensity can be rejected by the models shown in Figure 9, where the model phase dependences for large τ are completely inconsistent with observed phase dependence. Dust optical depths of 0.1 or less are strongly suggested.

We also note that the total obscuration of the nucleus will be the summation of that due to the dust boundary layer and that due to a jet which may extend beyond the boundary layer. However the jets are readily identifiable; their positions and brightness can be measured. If the number density within the boundary layer is inversely proportional to the dust velocity (condition of continuity) the dust ratio of the total columnar density can be obtained. Estimates of the optical thickness of dust in relatively clear regions of the VEGA-2 images is in the range, $0.1 < \tau < 0.3$. Thus, the optical thickness of the boundary layer must be very much less. We therefore conclude that the surface and limb of the nucleus seen in Figure 4 and much of that seen in Figure 5 is real and not an illusion created by jet or boundary layer dust.

5. The first successful steps have been accomplished to get a 3-d model of the nucleus. The software is now ready if the appropriate contours are provided. Provisionally, a 3-d model has been generated, but it uses contours satisfying only the criteria of 2.a. These preliminary results are already promising but will be published only after using limb fits that satisfy a variety of criteria.

DISCUSSION

First we summarize all the main results that the VEGA TVS experiment has yielded for the nucleus, including those published in /2/ and all the corroborative data from other experiences:

- Comet Halley has a solid, irregularly shaped nucleus with overall dimensions of $16 \times 8 \times 8$ km; it rotates in the direct sense with a period of 53 ± 2 h, about an axis that is nearly (within $5-10^\circ$) perpendicular to the orbit plane.
- The nucleus is covered by a very dark material, resulting in a low, 0.04 ± 0.01 albedo. The phase coefficient is about 0.05 mag/degree, and the color is essentially neutral.
- Jet activity varies with time; during the V-2 encounter the active zone formed at least one long quasi-linear feature on the surface.
- The dust layer covering the surface is optically thin, the surface was easily distinguishable through it. The surface is rough, probably as rough as the Moon's.
- Brightness variations on the surface, even very extended ones are distinguishable on processed images. Some of them could be topographical features, jet sources, etc. Other might be caused by dust-jet shadows or the optical variation of the dust layer. Only further analysis, done together with 3-d modelling will reveal their true nature, Figure 10.

Our conclusions regarding the nucleus are neither derived from nor enhanced by the published results of the HMC experiment. Other spaceborn experiments, with relevance to our analysis, have reached following conclusions:

- The Lyman- α imaging of the nucleus on Suisei /9/ confirmed both the 53 h rotation period, and that the nucleus is covered with hard substance; they identified two strong (S1, S2) and four weak (W1-W4) sources, resulting in a periodic breathing of the Lyman- α coma. The angular position of the sources are: S1(0°)-W1(20°)-W2(75°)- S2(150°)- W3(204°)- W4(326°); where the angles in paranthesis are the positions of the sources projected onto an arbitrary circle. They concluded that V-1 experienced the outburst of S2, whereas V-2 did the same with W4, assuming a 7h time-of-flight for dust particles from surface to s/c.

- Both PUMA on VEGA /10/ and PIA on Giotto /11/ confirmed that dust can be classified into three distinct classes, one is quite close to C1 carbonaceous chondrites, but at least 80% of the dust particles do not fall into this class. The overall carbon content is richer than is found in C1 c.c.

- The surface temperature measured by the infrared sounder on V-1 was 300-400 K° /12/. This is an important result because it shows that the nuclear surface cannot be highly darkened ice.

When the cometary missions were planned, Whipple's dirty snow ball model was generally accepted. It predicted fairly high albedo and more or less homogeneous dust and gas emission. The model was slightly improved by many authors, adding a mantle on top, /13/ introducing better chemistry /14/ etc. However, after the reanalysis of the 1910 apparition /15/ it was generally realized that jets contribute far more to the cometary atmosphere than had been assumed and their analysis pointed to the presence of linear sources on the surface.

This conclusion was reinforced by the VEGA imaging experiment, as well as by the Lyman- α detector on Suisei. The imaging data revealed a solid surface. Hence, the line sources could have been formed either when the comet was formed by gluing large subunits together, or more likely, that they have been created by thermal stresses near the surface. The thermal stresses should be high, since the surface temperature is high, as measured by IKS on VEGA. It is interesting to point out that in spite of the elevated surface temperature the jet phenomena are short lived, and they are present only when the Sun illuminates the source. No significant amount of dust was observed behind the terminator. This suggests a low heat conductivity in the surface. Due to low conductivity, it should remain quite hot even on the dark side. As little or no dust was observed there, a possibility is a solid surface, generally impervious to the escape of gas, where even the volatiles are mostly produced from the jet sources. Another possible structure of the surface is ice covered by some thin layer of dark material with low thermal conductivity. The high surface temperature and low albedo coincides very well with the high carbon content observed by the dust experiments. It had been considered from the low albedo that the surface is covered by carbon-rich ice; however, this contradicts both to high surface temperature and to the very concentrated matter emission and the lack of activity on the night side, not even shortly after sunset.

The dust mass spectrometer observed three different classes of dust. It would have been very interesting to know whether in time the classes were separated somehow, or were always segregated. The high carbon content of the dust and the above mentioned properties of the surface allows us to suggest that the dust observed is not very different from the surface material. The brightness variations observed on the surface from different viewing geometries do not exclude chemical variations, but they may also be explained by elevation variations or dust-jet shadows. The intensity variations of the jet activity is probably connected to surface topography. The 3-d modeling could provide an answer to this.

It was important to conclude from the low optical thickness of the near surface dust layer and from the phase variations that the surface is rough, perhaps similar to the Moon, though it is very likely that more detailed photometric studies will reveal some differences. By the analysis of nuclear phase function and photometric profiles, at least some classes of surface materials can be excluded. It would be interesting to examine how much of the non-jet-emitting surface, subjected to cosmic rays, etc. is characteristic of the general composition.

When comets were formed, probably some large ones were formed as well. For many of them, there is some likelihood that one of the primitive giant planets would capture them as a satellite. It can not be excluded at this stage that Umbriel, a satellite of Uranus observed recently by Voyager, is very similar to Halley, albeit much larger.

In summary we think that the dusty snow-ball model will undergo modifications in the future. The extent of that is difficult to judge before analyzing in more detail all the results of the cometary missions.

REFERENCES

1. L. Szabo, G.A. Avanesov, P. Cruvellier, I.U. Barinov, G.I. Cukanova, M. Dettaille, M. Gárdos, T. Gombosi, V.I. Kostenki, T. Nguyen, I. Rényi, R.Z. Sagdeev, S. Szalai, V.I. Tarnopolskij, M. Zseni, Television system for the Venus-Halley mission, in Cometary Exploration, Vol.3. ed. T. Gombosi, Central Research Institute for Physics, Budapest, 1983, p. 266.
2. R.Z. Sagdeev, F. Szabo, G.A. Avanesov, P. Cruvellier, L. Szabo, K. Szegő, A. Abergel, A. Balazs, I.U. Barinov, J.-L. Bertaux, J. Blamont, M. Dettaille, E. Demarellis, G.N. Dul'nev, G. Endrőczy, M. Gárdos, M. Kanyo, V.I. Kostenko, V.A. Krasikov, T. Nguyen-Trong, Z. Nyitrai, I. Rényi, P. Rusznyák, V.A. Shamis, B.A. Smith, K.G. Sukhanov, F. Szabo, S. Szalai, V.I. Tarnopolsky, I. Toth, G. Tsukanova, B.I. Valnicek, L. Varhalmi, Yu.K. Zaiko, S.I. Zatsepin, Ya.L. Ziman, M. Zseni, B.S. Zhukov, Television observations of comet Halley from Vega spacecraft, NATURE, 321, 262-266 (1986)
3. R.Z. Sagdeev, B.A. Smith, K. Szegő, A. Kondor, V.A. Kvasikov, S. Larson, V.A. Shamis, V.I. Tarnopolski, I. Toth, The spatial distribution of dust jets seen by V-2, KFKI-1986-39, Central Research Institute for Physics, Budapest
4. O.L. Vaisberg, V.N. Smirnov, L.S. Gonn, M.V. Iovlev, M.A. Balikchin, S.I. Klimov, S.P. Savin, V.D. Shapiro, V.I. Shevchenko, Dust coma structure of comet Halley from SP-1 detector measurements, NATURE, 321, 274-276 (1986)
5. N. Divine, H. Fechtig, T.I. Gombosi, M.S. Hanner, H.U. Keller, S.M. Larson, D.A. Mendis, R.L. Newburn Jr., R. Reinhard, Z. Sekanina, D.K. Yeomans, The Comet Halley dust and gas environment, Cometary Sci. Team, No. 72, Jet Propulsion Laboratory, (1985)
6. E.P. Mazets, R.L. Aptekar, S.V. Golenetskii, Yu.A. Guryan, A.V. Dyachkov, V.N. Ilyinskii, V.N. Panov, G.G. Petrov, A.V. Savvin, R.Z. Sagdeev, I.A. Sokolov, N.G. Khavenson, V.D. Shapiro, V.I. Shevchenko, Comet Halley dust environment from SP-2 detector measurements, NATURE, 321, 276-278, (1986)

7. J.A.M. McDonnell, W.M. Alexander, W.M. Burton, E. Bussoletti, D.H. Clark, R.J.L. Grand, E.Grun, M.S. Hanner, D.W. Hughes, E. Igenbergs, H. Kuczera, B.A. Lindblad, J.-C. Mandeville, A. Minafra, G.H. Schwehm, Z. Sekanina, M.K. Wallis, J.C. Zarnecki, S.C. Chakaveh, G.C. Evans, S.T. Evans, J.G. Firth, A.N. Little, L. Massonne, R.E. Olearczyk, G.S. Pankiewicz, T.J. Stevenson, R.F. Turner, Dust density and mass distribution near comet Halley from Giotto observations, NATURE, 321, 338-341, 1986.
8. H.U. Keller, C. Arpigny, C. Barbieri, R.M. Bonnet, S. Cazes, M. Coradini, C.B. Cosmovici, W.A. Delamere, W.F. Huebner, D.W. Huges, C. Jamar, D. Malaise, H.J. Reitsem, H.U. Schmidt, W.K.H. Schmidt, P. Seige, F.L. Whipple, K. Wilhelm, First Halley multicolour camera imaging results from Giotto, NATURE, 321, 320-326, 1986.
9. E. Kaneda, O. Ashihara, M. Shimizu, M. Takagi, K. Hirao, Observation of comet Halley by the ultraviolet imager of Suisei, NATURE, 321, 297-299, 1986.
10. J. Kissel, R.Z. Sagdeev, J.L. Bertaux, V.N. Angarov, J. Audouzel, J.E. Blamont, K. Buchler, E.N. Evlanov, H. Fechtig, M.N. Fomenkova, H. von Hoerner, N.A. Inogamov, V.N. Khoromov, W. Knabe, F.R. Krueger, Y. Langevin, V.B. Leonas, A.C. Levasseur-Regourd, G.G. Managadze, S.N. Podkolzin, V.D. Shapiro, S.R. Tabaldyev, B.V. Zubkov, Composition of comet Halley dust particles from Vega observations, NATURE, 321, 280-282, 1986.
11. J. Kissel, D.E. Brownlee, K. Buchler, B.C. Clark, H. Fechtig, H. Grün, K. Hornung, E.B. Igenbergs, E.K. Jessberger, F.R. Krueger, H. Kuczera, J.A.M. McDonnell, G.M. Morfill, J. Rahe, G.H. Schwehm, Z. Sekanina, N.G. Utterback, H.J. Volk, H.A. Zook, Composition of comet Halley dust particles from Giotto observations, NATURE, 321, 336-337, 1986.
12. M. Combes, V.I. Moroz, J.F. Crifo, J.M. Lamarre, J. Charra, N.F. Sanko, A. Soufflot, J.P. Bibring, S. Cazes, N. Coron, J. Crovisier, C. Emerich, T. Encrenaz, R. Gispert, A.V. Grigoryev, G. Guyot, V.A. Krasnapolsky, Yu.U. Nikolsky, F. Rocard, Infrared sounding of comet Halley from Vega-1, NATURE, 321, 266-268, 1986
13. M. Horányi, T.I. Gombosi, T.E. Cravens, A. Körösmezey, K. Kecskemety, A.F. Nagy, K. Szegő, The friable sponge model of a cometary nucleus, Astrophysical J., 278, 449-455, 1985
14. D.A. Mendis, H.L.F. Houppis, M.L. Marconi, The physics of comets, Fundamental of Cosmic Physics, 10, 1-380, 1985.
15. S.M. Larson, Z. Sekania, Coma morphology and dust-emission pattern of periodic comet Halley, Astr. J., 89, 571-578, 1984.

Table 1.

	Narrow angle camera	Wide angle camera	
Focal length, mm	1200	150	
Diameter, mm	240	50	
Relative aperture	1:5, eff. 1:6.5	1:3	
Number of imaging channels	2	2	
Spectral filters	8 filters in the 400-1100 nm range	fixed filter 630-760 nm	fixed filter 630-760 nm Set of 7 filters 630-760 nm, and one, 400-1100nm
Exposure range	0.01 to 163 s	6 ms to 800 ms	
Angular field of view (min. of arc)	26.4x39.6	211x316	211x118
Comet detection criterion	Identification of the brightness maximum within the brightest portion of the image with corrections for individual characteristics of image detectors	Identification to the brightness maximum of the brightest area of the Comet	
Housekeeping and video data transmission via the high-data-rate radio link	8-bit code or 12-bit nonproof code, at a rate of 32 kbit/s		

TABLE 1 The principal characteristics of the VEGA imaging system

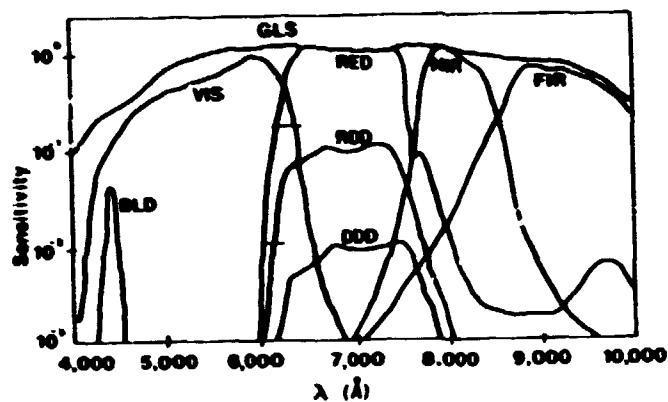


Fig. 1. The spectral sensitivity of the scientific imaging telescope, for different filters used.

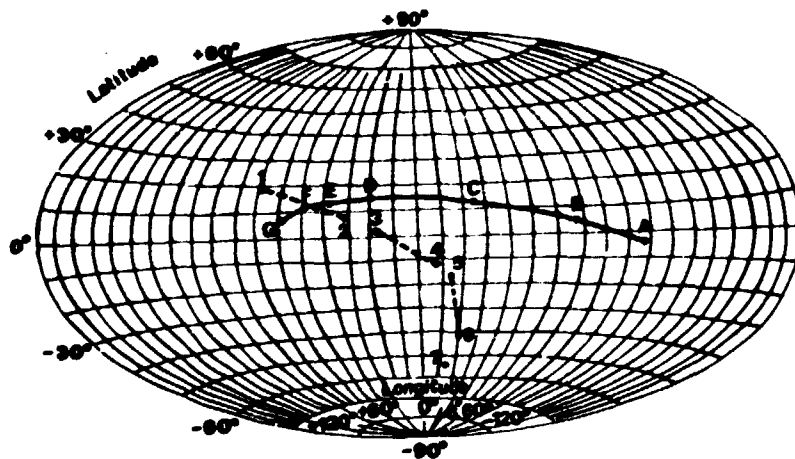
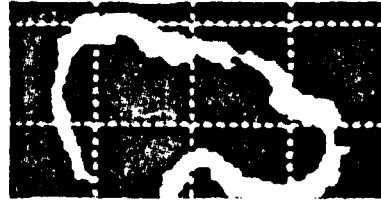
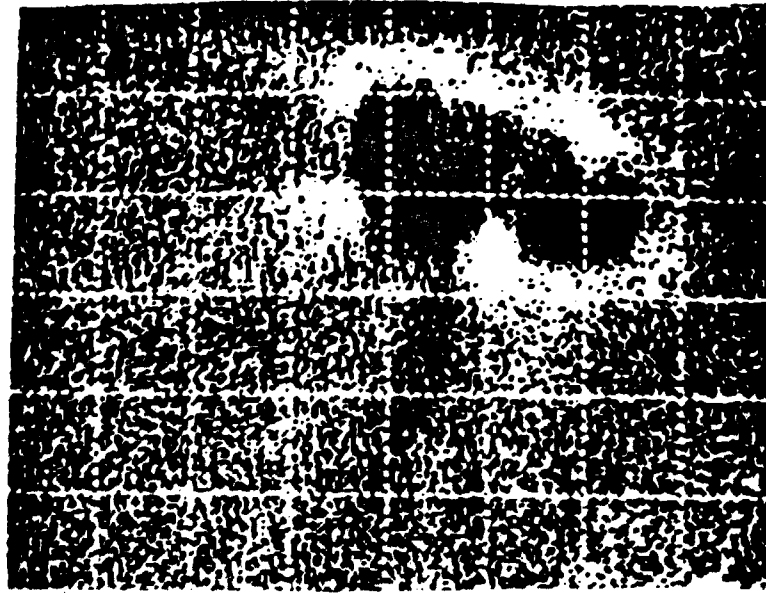


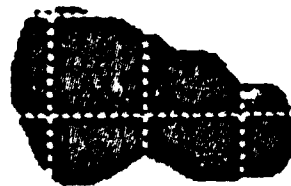
Fig. 2. The path of VEGA-2 projected onto a sphere centered on the nucleus. North is ecliptic north on the figure, the subsolar point defines zero longitude. On the path, dots indicate the recording of the images; e.g. we list for images A-G the recording time relative to encounter (E) and distance from the nucleus. (A: E-370.5 sec, 29539 km; B: E-101.7 sec, 11197 km; C: E-1.5 sec, 8031 km; D: E+98.7 sec, 11037 km; E: E+187.3 sec, 14462 km; F: E+280.5 sec, 22971 km; G: E+558.1 sec, 43567 km). The identified line-like jet sources are denoted by 1-2, 3-4 and 5-6, point sources are 7 and 8.



3a)



3b)

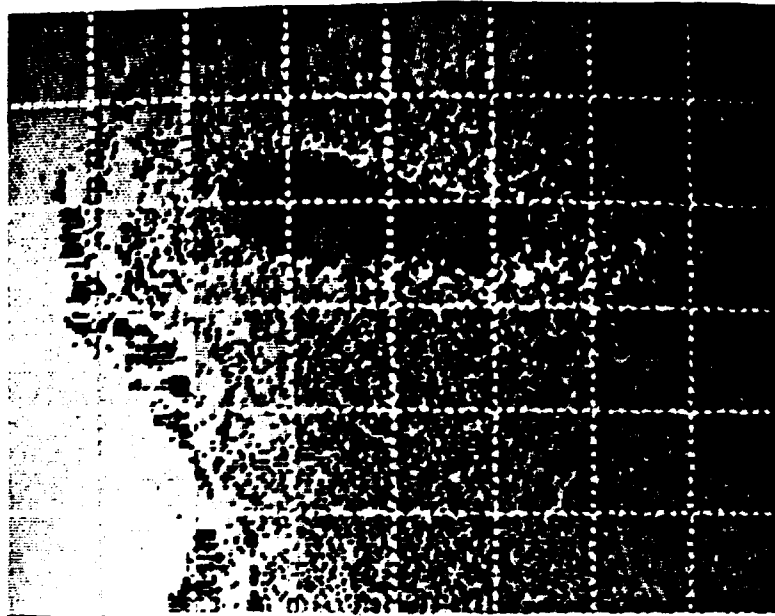


3c)

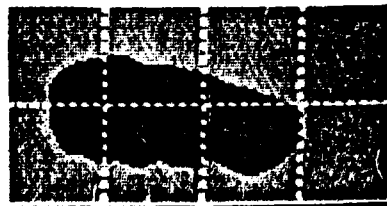
Fig. 3. Solution for the limb of image C in Fig. 2.



4a)



4b)



4c)

Fig. 4. Solution for the limb of Image D in Fig. 2

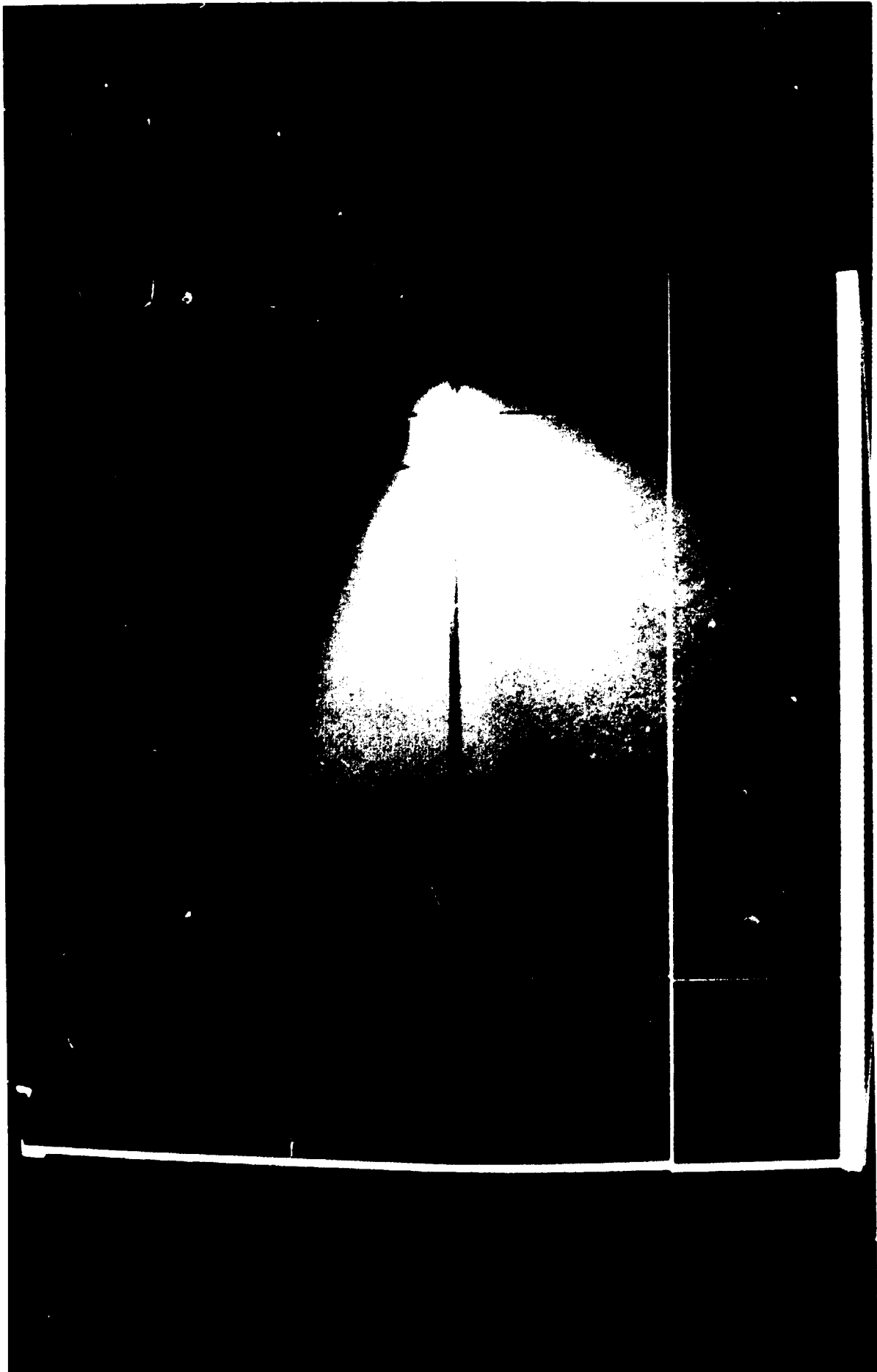


1190



1194

Fig. 5. Size corrected, preprocessed images C and D.



1185

Fig. 6. Raw image B in Figure 2. The nuclear region is overexposed. The broad fan-like jet extending to the lower left, for example, is from the linear source 5-6 in Figure 2.

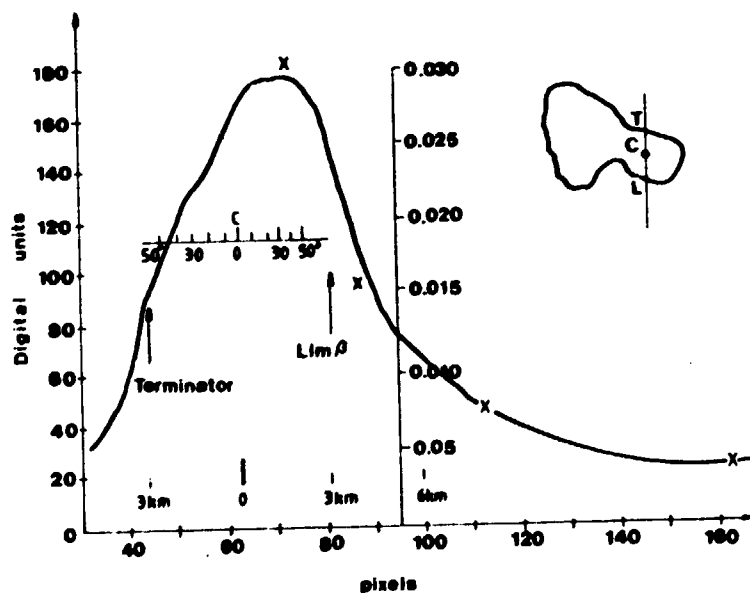


Fig. 7. An example of the photometric profile of image C averaged from five pixels columns. An approximation of brightness outside of the boundaries of the nucleus by the relationship, $\rho \propto 1/r$, is given by crosses; α is emission angle.

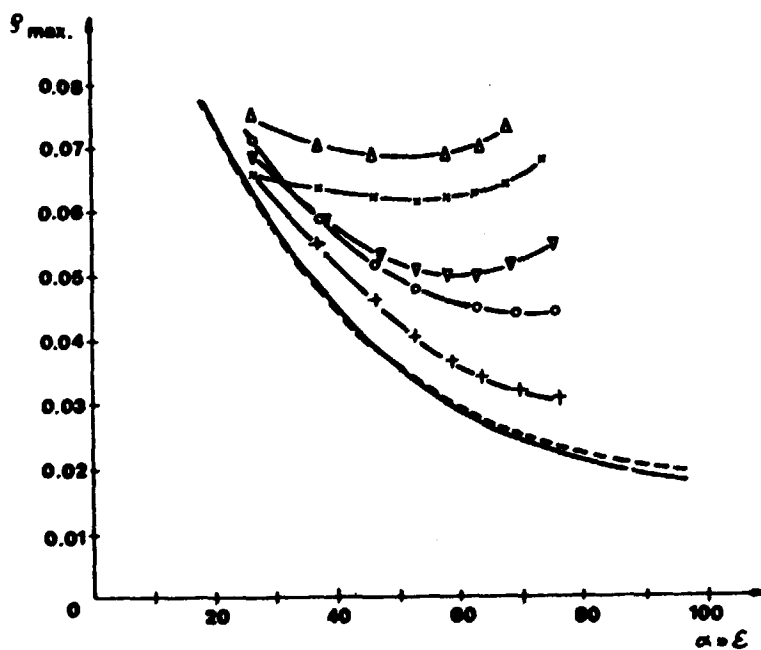


Fig. 8. A comparison of model photometric profiles (see Figure 7) with the observed profile; ϵ = emission angle, i = incidence angle (calculated by the approximation that surface along line L-T on Figure 7 is a spherical segment with center in C). The thick full line: measured ρ ; dashed line: model ρ , without dust; model profiles with dust are for (+) $\tau = 0.1$; (O) $\tau = 0.2$; (Δ) $\tau = 0.4$; (x) $\tau = 1$; (δ) $\tau = 2$. The lower values (Δ) are half those of the model for $\tau = 2$ (see text). The phase angle is 28° and the value of the phase function $x(\alpha)/4\pi = 0.042$ was used here.

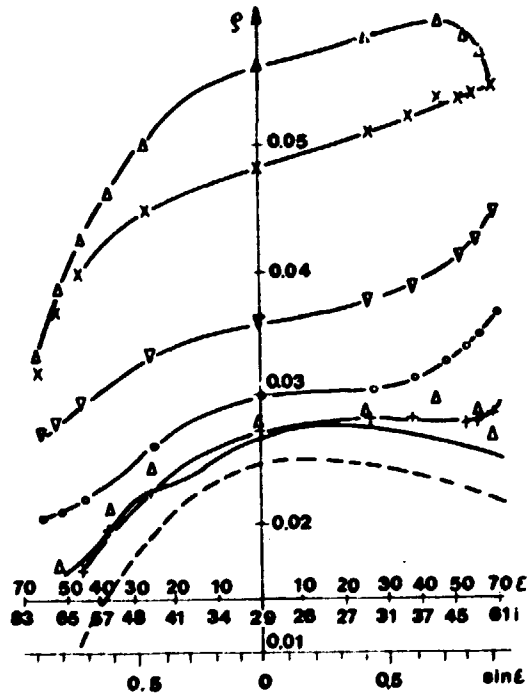


Fig. 9. Phase dependence of the brightest point on images of the nucleus obtained by VEGA-1; full line : measurements /4/; dotted line : model of ρ_s for a lunar-like surface. Other symbols are the same as for Figure 8. Difference in measured ρ_{\max} with Figure 7 can be a consequence of calibration errors. Model ρ_s for the lunar-like surface model here is different from that in Figure 8 due to renormalization.

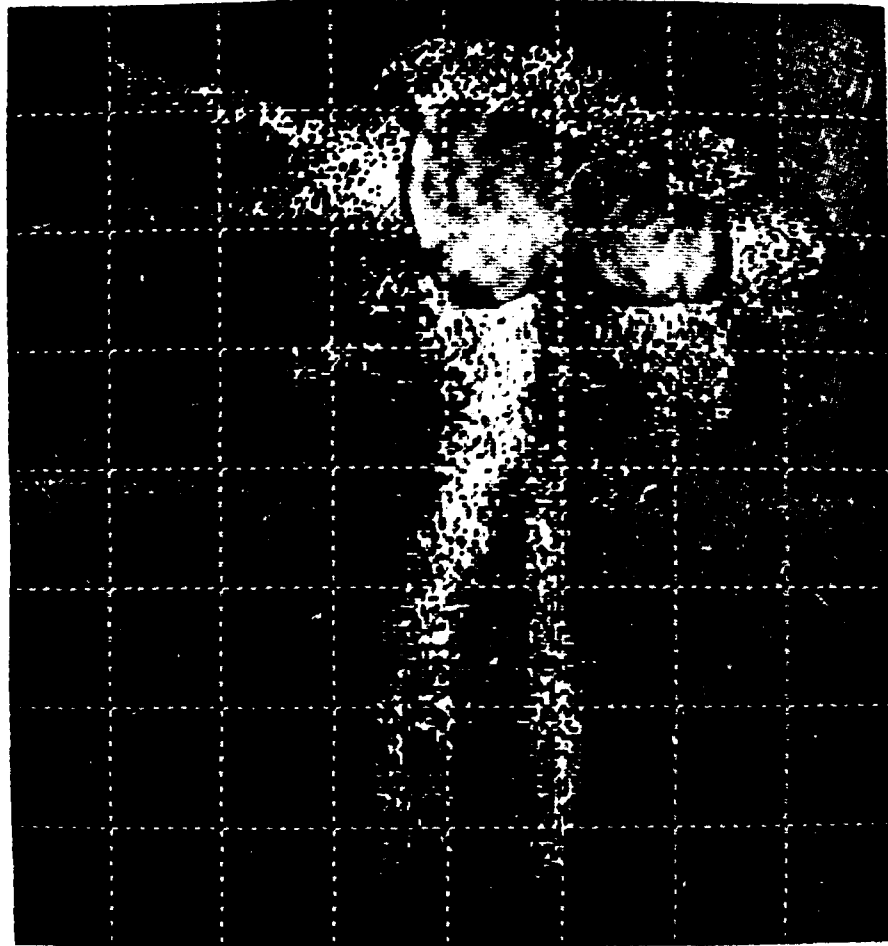


Fig. 10. Brightness variations on image C.

The issues of the KFKI preprint/report series are classified as follows:

- | | |
|-----------------------------------------------------------|--------------------------------------------------------------------------|
| A. Particle and Nuclear Physics | H. Laboratory, Biomedical and Nuclear Reactor Electronics |
| B. General Relativity and Gravitation | I. Mechanical, Precision Mechanical and Nuclear Engineering |
| C. Cosmic Rays and Space Research | J. Analytical and Physical Chemistry |
| D. Fusion and Plasma Physics | K. Health Physics |
| E. Solid State Physics | L. Vibration Analysis, CAD, CAM |
| F. Semiconductor and Bubble Memory Physics and Technology | M. Hardware and Software Development, Computer Applications, Programming |
| G. Nuclear Reactor Physics and Technology | N. Computer Design, CAMAC, Computer Controlled Measurements |

The complete series or issues discussing one or more of the subjects can be ordered; institutions are kindly requested to contact the KFKI Library, individuals the authors.

Title and classification of the issues published this year:

- | | |
|---------------------------------------|--------------------------------------------------------------------------------------------------------------------------------------------------------------------------------------|
| KFKI-1986-01/E
J. Kollár et al. | The Kronig-Penney model on a Fibonacci lattice |
| KFKI-1986-02/C
A.J. Somogyi et al. | First results of high energy particle measurements with the TÜNDE-M telescopes on board the S/C VEGA-1 and -2 |
| KFKI-1986-03/C
K. Gringauz et al. | The VEGA PLASMAG-1 experiment: description and first experimental results |
| KFKI-1986-04/A
J. Révai | Half-classical three-body problem |
| KFKI-1986-05/A
I. Lovas | Quark degrees of freedom in nuclei |
| KFKI-1986-06/E
Gy. Szabó et al. | Lattice gas model on tetrahedral sites of bcc lattice: anisotropic diffusion in the intermediate phase |
| KFKI-1986-07/K
Pálfalvi J. et al. | Tapasztalatok egy (neutron-alfa) magreakción alapuló szilárdtest nyomdetektorokból felépített személyi albedo neutron doziméter munkaszintű dozimetriai felhasználásáról |
| KFKI-1986-08/K
Nagy Gy. et al. | Összefoglaló értékelés a paksi környezetellenőrző rendszer GM-csőves és jódtáv mérő detektorainak jellemzőiről az 1982-1985-ös mérési adatok feldolgozása alapján. OKKFT-A/11-7.5.9. |
| KFKI-1986-09/K
Nagy Gy. et al. | A paksi atomerőmű hideg- és melegvizcsatornájában üzemelő folyamatos vizaktivitás monitorok paramétereinek és mérési adatainak összefoglaló értékelése. OKKFT-A/11-7.4.13. |
| KFKI-1986-10/D
S. Zoletnik et al. | Determination of the centre of gravity of the current distribution in the MT-1 tokamak |

KFKI-1986-11/G R. Kozma et al.	Studies to the stochastic theory of the coupled reactor-kinetic-thermohydraulic systems. Part VI. Analysis of low-frequency noise phenomena
KFKI-1986-12/A A. Frenkel	Canonical quantization of the relativistic theory of the Dirac monopole
KFKI-1986-13/D Gy. Egely	Energy transfer problems of ball lightning
KFKI-1986-14/K Németh I. et al.	Hordozható félvezető gamma-spektrométer üzembe állítása, kalibrálása, számítógépes adatfeldolgozása és tesztelése in situ dózisteljesítmény meghatározás céljából. OKKFT-A/11-7.4.12.
KFKI-1986-15/G M. Makai	In aid of in-core measurement processing
KFKI-1986-16/C K.I. Gringauz et al.	First in situ plasma and neutral gas measurements at comet Halley: initial VEGA results
KFKI-1986-17/C A.J. Somogyi et al.	First spacecraft observations of energetic particles near comet Halley
KFKI-1986-18/E Z. Kaufmann et al.	Unusual maps and their use to approach usual ones
KFKI-1986-19/A H-W. Barz et al.	Effect of correlations on entropy and hadro-chemical composition in heavy ion reactions
KFKI-1986-20/B A. Horváth et al.	Evidence for a different miocene solar cycle?
KFKI-1986-21/M D. Nicholson	On the humanisation of interfaced systems
KFKI-1986-22/L Novothy F. et al.	Kísérlet mérőváltók meghibásodásának zajdiagnosztikájára 2.
KFKI-1986-23/C T.I. Gombosi et al.	An icy-glue model of cometary nuclei
KFKI-1986-24/A P. Lévai et al.	Should the coupling constants be mass dependent in the relativistic mean field models?
KFKI-1986-25/E G.P. Djotyan et al.	Theory of the nonstationary phase conjugation by four-wave mixing
KFKI-1986-26/E P. Szépfalussy et al.	A new approach to the problem of chaotic repellers
KFKI-1986-27/J A. Vértés et al.	Peak shape determination in laser microprobe mass analysis
KFKI-1986-28/E P. Fazekas	Variational ground state for the periodic Anderson model
KFKI-1986-29/A V.N. Gribov	A new hypothesis on the nature of quark and gluon confinement
KFKI-1986-30/A L. Diósi	A universal master equation for the gravitational violation of quantum mechanics

KFKI-1986-31/D
J.S. Bakos

Optically pumped FIR lasers and their application in
plasma diagnostics

KFKI-1986-32/B
Zs. Bagoly et al.

Monopole abundance from first order gut phase
transition of the early universe

KFKI-1986-33/B
Z. Perjés

Ernst coordinates

KFKI-1986-34/C
R.Z. Sagdeev et al.

Comet Halley: Nucleus and jets (Results of the VEGA
mission)

Kiadja a Központi Fizikai Kutató Intézet.
Felelős kiadó: Szegő Károly
Szakmai lektor: Varga András
Nyelvi lektor: Bencze Gyula
Példányszám: 620 Törzsszám: 86-407
Készült a KFKI sokszorosító üzemében
Felelős vezető: Tőrekői Béláné
Budapest, 1986. június hó